Journal of the Indian Institute of Science
A Multidisciplinary Reviews Journal
ISSN: 0970-4140 Coden-JIISAD

REVIEWS

Visualization and Image Processing of Compressible Flow in a Supersonic Gaseous Ejector

M.V. Srisha Rao and G. Jagadeesh

Abstract | A supersonic ejector is an aerodynamic device used as a compressor/vacuum generator/gas mixer, simple in construction, having varied applications. It is, however, complex in its flow structure. Flow visualization techniques are essential to understand flow dynamics in general, and with modern image processing techniques their utility has been enhanced to evaluate field data of the flow. To understand the gas dynamics in an ejector multiple visualization tools that compliment each other have been implemented including time resolved schlieren and laser scattering from acetone particles seeded in the primary flow. While schlieren emphasizes flow features by density gradient created due to the flow, the need to clearly distinguish the primary and secondary flow from one another necessitates the use of seeding and laser scattering. The primary objective is to use two flow visualization techniques to clearly capture the flow within a supersonic ejector followed by analysis of the images by digital image processing tools to compute the non-mixed length. Following a brief review of flow visualizations and the supersonic ejector, experimental techniques and details of the visualization procedures are described in the paper. Instantaneous flow images at two operating conditions of primary stagnation pressure at 9.69 bar and 5.69 bar are presented, and their qualitative inferences are described. The image processing tools of MATLAB have been used to develop algorithms that enhance the quality of raw images and through the definition of appropriate criteria by using intensity profile along the height of the ejector, quantitative inferences on non-mixed length is made from both the schlieren and laser scattering images. For the case with primary stagnation pressure of 9.69 bar the length of non-mixed region is evaluated as 4.65 L/D from the laser scattering and 4.95 L/D from schlieren techniques. Given the sources of errors and uncertainity of 6% both the methods of visualizations give results in agreement with each other.

1 Introduction

1.1 *The supersonic ejector*

A supersonic ejector is an aerodynamic device which consists of a supersonic nozzle within a variable area mixing duct followed by an expanding diffuser, as shown diagrammatically in Figure 1. The expanding primary flow generates a suction for the secondary flow that causes entrainment of secondary flow followed by mixing of the two flows in the mixing duct; the mixed flow then undergoes a pressure recovery in the diffuser, thereby the

Department of Aerospace Engineering, Indian Institute of Science, Bangalore 560012, Karnataka, India.
jagadeeshgopalan@gmail.com

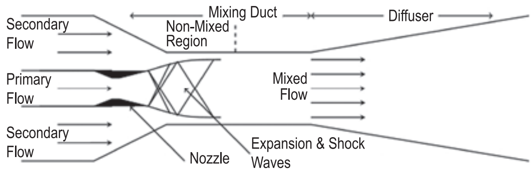

Figure 1: Schematic diagram of the flow through a generic ejector.

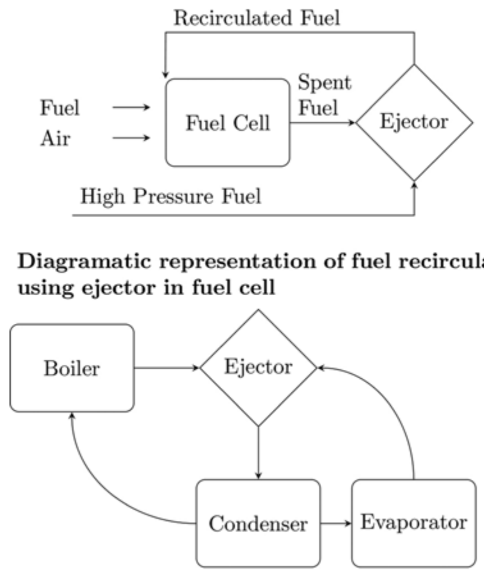

Diagramatic representation of fuel recirculation using ejector in fuel cell

Diagramatic representation of a refrigeration cycle with ejector

Figure 2: Application of ejector in fuel cells and refrigeration.

secondary flow is pumped by using momentum and energy augmentation from the primary flow. A supersonic flow has velocities greater than the local speed of sound, consequently limitations on propagation of acoustic waves compared to the flow velocity causes development of shock waves and expansions, which are regions of sharp changes in velocity and thermodynamic properties of the flow in response to changes in the flow condition.[1] The interface of two flows with different velocities dominated by shear forces is referred to as the mixing layer, which in this case is turbulent, compressible and subjected to large pressure gradients. These devices are simple in construction and operate without any moving parts, proving advantageous in many applications where conventionally compressor/vacuum pumps are used. The ejectors have been explored for alternate green refrigeration cycles.[2–4] Fuel cells are promising power generators for future, and the ejector finds a role in recirculation or purging of spent fuel.[5] Figure 2 is a simple diagrammatic representation of the part played by the ejector in these applications. These devices have also found applications for thrust augmentation,[6–8] noise reduction in jets, condenser vacuum generation in power plants and in aerodynamic testing installations.[9,10]

The operation and control of the ejector is solely based on gas dynamic phenomena caused by the interactions of the supply conditions—stagnation pressures and temperatures and the geometry. Experimental, analytical and numerical tools have been used to understand, model and design the ejector. Experimental investigations have mostly focused on generating the operating regimes of the flow by pressure measurements and flow rate measurements.[11–13] The analysis of ejectors using control volume techniques leading to design methodologies and optimization can be found in some of the earlier work.[13–16] Numerical simulations of the flow through ejectors have also been reported in the open literature.[17] Fundamental to the operation of the ejector are the dynamics of a supersonic jet with a co-flow that is confined between variable area walls. The mixing layer that develops between both flows is largely turbulent and compressible in nature, and is subjected to large pressure gradients due to shocks within the supersonic jet as well as the varying area presented by the confinement of the walls. Understanding gas dynamics of the mixing process under such conditions holds the key to understanding and improving the performance of the supersonic ejector. While turbulent mixing layer has been studied using schlieren, shadowgraphs[18,19] and techniques like Planar Laser Mie Scatterring,[20] the configuration resembles an open domain flow with bounding walls far away from the jet core, unlike the ejectors where the jet is closely bounded by a co-flow and walls of the mixing duct. Schlieren images of the flow through the ejector can be found in,[11,21] however, they lack in efforts to quantitatively estimate parameters of flow from the image. Laser based visualizations of the ejector flow and image analysis to estimate mixing has been attempted for a few generic conditions.[22,23] From what is available in open literature it is evident that criteria to determine the mixing length in an ejector is a matter of ongoing interest and with immense design utility. The flow through the ejector is sufficiently complex, involving a mixture of subsonic, supersonic regimes of flow, shocks, compressible mixing layers and boundary layers that a comprehensive understanding requires use of multiple methods of optical diagnostics. Two complimentary optical tools have been used to study the flow through the supersonic ejector—the time-resolved schlieren and the laser scattering method. The images captured are further processed by digital image processing algorithms to arrive at quantitative estimates of the mixing within the ejector.

1.2 *Flow visualization*

Primary interest of a fluid dynamicist lies in understanding the fluid flow phenomenon by knowing the flow parameters at all locations of space and instants of time. Conventional measurement techniques like pressure, temperature sensors, velocity anemometers, and pitot probes are point measurement devices that are intrusive in nature and require tedious traverse mechanisms followed by data analysis to construct the flow field. It is in this context that flow imaging using different flow visualization techniques gain significance since they can yield field information and the structures in the flow are immediately apparent. Merzkirch[24] has a comprehensive collection of various flow visualization techniques and their applications to different flow scenarios. Gases are transparent, however their flows are generally compressible leading to density gradients in the flow, that have been exploited in schlieren and shadowgraph techniques which have been described in detail by Settles.[25] The introduction of lasers into flow visualizations has spawned methods like interferometry, Particle Image Velocimetry (PIV), and Laser Induced Fluorescence (LIF). The advances in CCD and CMOS technologies has lead to digital cameras of increasingly better spatial and temporal resolutions. Digital recording has been instrumental in revolutionizing visualization techniques as it becomes easier to conduct off-line image processing in computers enabling quantitative estimation of flow parameters from what would otherwise be qualitative images. Figure 3 shows the basic principle of two different kinds of visualization techniques, the first has a parallel beam of light incident into the flow region, the density gradients cause deflections of this light beam which is captured by camera; shadowgraph and schlieren techniques are based on this principle. The second method has the flow seeded with particles that scatter a sheet or beam of laser light, the scattered light is recorded by a camera; laser scattering makes use of this principle. While schlieren emphasizes the sharper features in the flow that generate high density gradients, the mixing of the two flows is not directly evident. Seeding the primary flow and using laser scattering helps monitor progress of mixing, the shock trains are less visible. Thus this work combines the two methods and image processing tools to arrive at a method for estimating the mixing in the ejector.

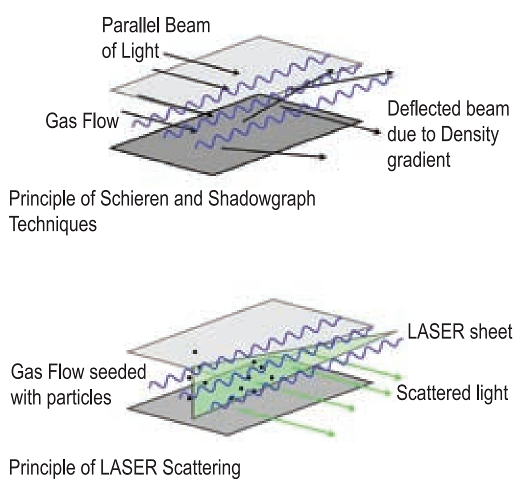

Figure 3: Schematic illustration of two kinds of flow visualization techniques.

1.3 *Image processing*

Image processing has increasingly become an indispensable tool for enhancing the utility of flow visualization images. Good digital image recording and computer technology has only helped matters, a host of techniques like PIV, quantitative PLIF, and BOS rely predominantly on image processing. In this work image processing tools of MATLAB have been used.[26] A library of codes for specific image processing tasks with adequate documentation can be found at.[27] Using these tools algorithms that address the processing needs for the current problem have been developed in house. The problem in question is to find the non-mixed length within the ejector, which is the length in the duct for which the primary and secondary flows are distinct. Qualitatively it can be inferred from the images, however, to get numerical data digital image processing has been carried out on the images and based on a criterion of mixing defined here the non-mixed length is computed. The procedure for such an analysis and a result for specific case is presented here.

2 Experimental Setup

An ejector test rig facility has been designed, fabricated and installed at the Laboratory of Shockwaves and Hypersonic Research (LHSR), Indian Institute of Science. The schematic diagram of the flow facility is shown in Figure 4. The facility has two compressed air tanks of 3 m^3 capacity at pressure of 12.5 bar which supply the primary flow. The primary flow is controlled by a pressure regulator and solenoid valve assembly. The primary flow is led from the tanks to a stagnation chamber where the stagnation pressure of the primary flow is measured after which it enters the ejector through a convergent divergent nozzle of

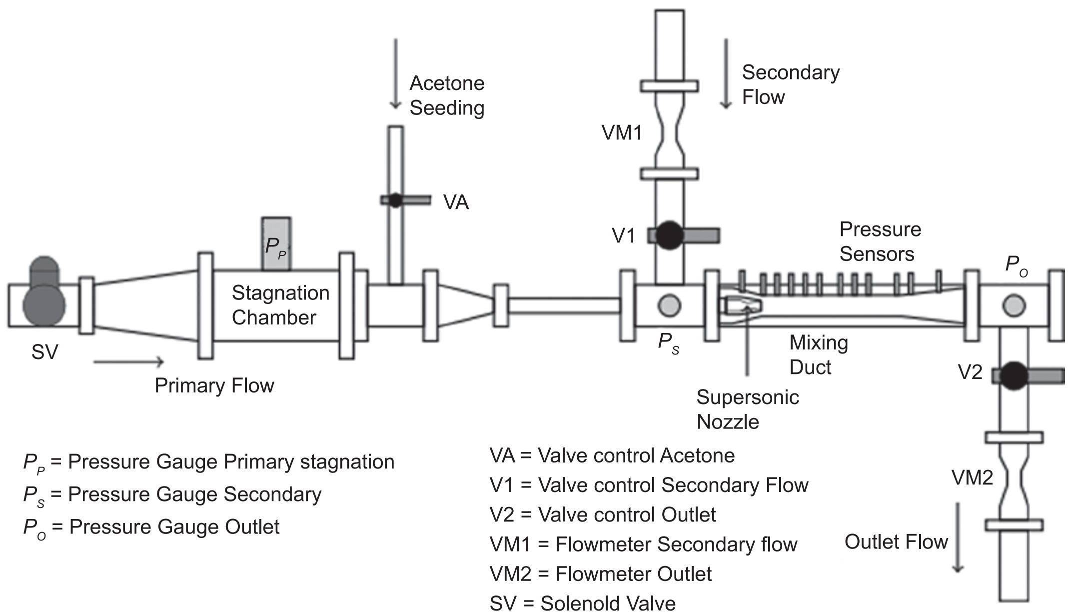

Figure 4: Diagrammatic representation of the ejector test facility.

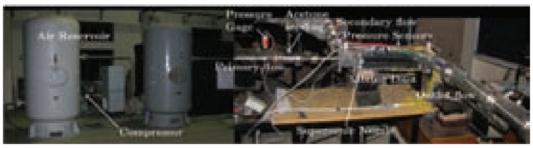

Figure 5: Photograph of the ejector test rig facility at LHSR.

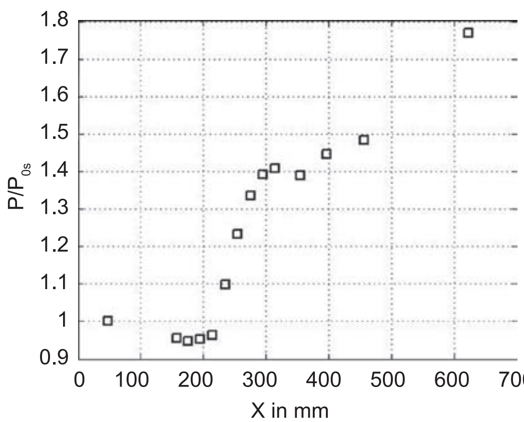

Figure 6: Static pressure profile along the ejector.

an exit Mach number of 2.48, and exit height of 6 mm. The constant area of the mixing duct has a height of 20 mm, giving an area ratio of 3.33 for the ejector. The secondary flow is entrained from the ambient atmosphere passing through venturimeter where the flow rate is measured and then to a short reservoir where the stagnation pressure is measured, before entering into the mixing duct. The ejector walls are instrumented with 12 kulite pressure transducers that measure static pressure along the wall. The diffuser exit has a pressure monitoring station and a venturimeter that measures the outgoing flow rate. Difference between outgoing and secondary flow rate gives the primary mass flow rate. The ratio of secondary to primary mass flow rate is termed as the entrainment ratio. The data is acquired using a DEWETRON data acquisition system connected to a computer. The side walls are made of optical quality BK-7 glass that gives an optical axis along the length of the ejector. Figure 5 shows the photograph of the facility at LHSR.

Figure 6 shows the static pressure profile measured along the walls of the ejector for a case with primary stagnation pressure at 9.69 bar and entrainment ratio at 0.24. The suction caused by the primary flow followed by pressure recovery of the mixed flow within the facility follows that of a typical ejector.

3 The Schlieren Technique

Z-type schlieren is setup across the ejector. It essentially consists of two concave mirrors. The first concave mirror renders light from a point source into a parallel beam, which passes through glass windows of the ejector and is collected by the second mirror. The second mirror focuses the beam onto a knife edge and then into the camera which captures the images. Two plane mirrors are used to fold the optical path within the constrained space. During the flow, density gradients present

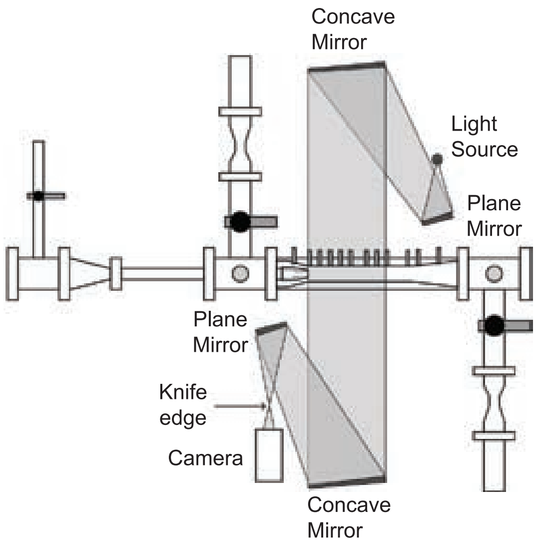

Figure 7: The schlieren arrangement for the ejector.

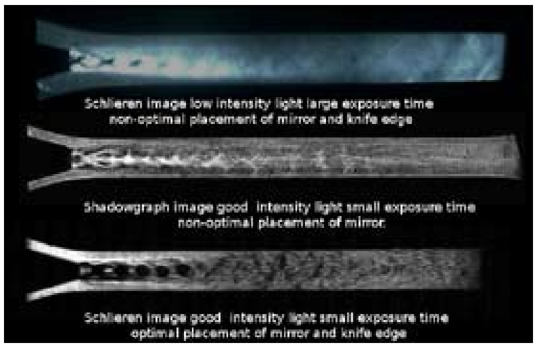

Figure 8: Series of schlieren images showing the improvement of quality of schlieren images with optical arrangements.

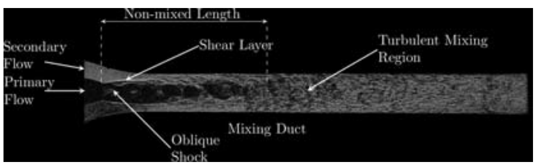

Figure 9: Instantaneous schlieren image of the flow at a primary stagnation pressure P_{op} of 9.69 bar and entrainment ratio $\omega = 0.24$.

within the flow cause deflections in the parallel beam of light. When the collected beam is cut by a knife edge at the focus, it acts like a filter allowing deflections in one direction to pass through and blocking the deflections in the other direction, thereby producing a gray scale image that is proportional to the density gradients in the flow. The optical set up uses mirrors of 30 cm diameter and focal length of 3 m for high sensitivity and sufficient viewing window. The position of knife edge is crucial for a good schlieren image, the direction of knife edge determines which gradients are being captured horizontal or vertical and consequently what flow features get highlighted. The knife edge is placed such that a uniform contrast is obtained prior to flow, and the setup is sensitive enough to pick up the thermal currents from a human hand. Since the dominant gradients in the flow are along the flow direction, i.e. horizontal, the knife edge is placed vertical. The Phantom v310 high speed camera is used to capture time resolved images at a resolution of 1024 × 800 and a frame rate of 2000 fps. Crisp images are obtained with lowest possible exposure times, however, this demands a very intense light source since exposure time and source intensity are contradictory objectives. A 250 W halogen lamp with focusing lenses is used as a light source which gives enough intensity to keep an exposure time of 6 μs. The best configuration of mirrors, light source and camera parameters were arrived after a series of experiments. Different light sources varying from a 3 W LED to the 250 W hologen lamp with collimating lenses were tried. The camera exposure time accordingly, was varied from milliseconds to the final 6 μs. Figure 8 shows the evolution of images from an initial non-optimal optical configuration to the best configuration. Figure 8 shows that when the light intensity is insufficient the exposure time has to be kept high to obtain an image of reasonable brightness and contrast. Consequently, the transient structures in the flow are averaged out and only the steady structures dominate, the overall contrast of the image is poor. The second image image shows a shadowgraph where no knife edge is used, here again the finer structures of the flow are not clearly visible. The third image shows the schlieren image at the best optical arrangement with a high intensity light source and low exposure time, showing crisp structures in the flow.

Figure 9 is an instantaneous schlieren image of the flow through the ejector at a primary stagnation pressure P_{op} = 9.69 bar and the entrainment ratio ω = 0.24. The expansion of primary supersonic jet with alternate shock and expansion regions are clearly visible. The secondary flow is subsonic and has very small density gradients, hence is seen as a bright region around the primary jet. The sharp interface—shear layer between the two flows is visible as a bright curve, the thickness of which grows with distance from the nozzle and ultimately, the two flows merge into a region of turbulent mixing. The mixed flow then moves into the diffuser, and the absence of any shock structures in the mixed flow implies that the flow has become subsonic after mixing. The length of region within the duct where two flows are seen distinctly is termed as the non-mixed region. The schlieren is just an image of density gradients and apriori knowledge of the occurrence of mixing leads to the qualitative interpretation.

3.1 *Image processing of schlieren images*

The schlieren images are analysed using image processing tools of MATLAB. Algorithms are developed and coded in order to extract the non-mixed length. From Figures 9 and 8, it can be observed that at the region near the exit of the nozzle, the two flows are distinctly separated by a shear layer within which the primary flow shock structure exists, and outside the subsonic secondary flow region is clear. Progressing along the length of the ejector the edge of the shear layer extends closer to the wall and the image generates line like features due to vortical structures and the mixing region is full of criss-cross lines. Hence when a high frequency filter is used which emphasizes line like structures, the density of lines increases downstream. This fact is used to compute the non-mixed length. The line structures are enhanced using the canny algorithm which is an edge detection algorithm. Figure 10 shows the edge detected image corresponding to the image in Figure 9. Notice the increase in density of lines at the turbulent mixing region.

The density of lines can be computed by taking an intensity profile along the vertical direction. Figure 11 is superimposition of a few lines on Figure 9 for which intensity profile plots are shown.

Figure 12 is an intensity profile plot at a location 5 mm from the exit of the nozzle. The peaks correspond to lines that may denote the shear layer or shocks as marked in the figure. Figure 13 shows the progress of the intensity profiles along the ejector, more the number of peaks, more the lines. A criterion for the length of non-mixed length can be arrived at by taking a ratio of the vertical number density of lines at a particular x location to the maximum vertical number density in all of the ejector, using which the non-mixed length is computed to be 99 mm which is 4.95 L/D for this

Figure 10: Edge enhanced schlieren image using the canny algorithm.

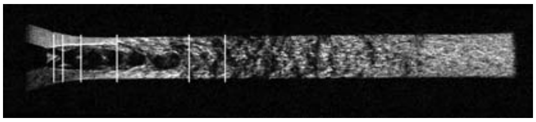

Figure 11: Lines along which the intensity profiles are plotted.

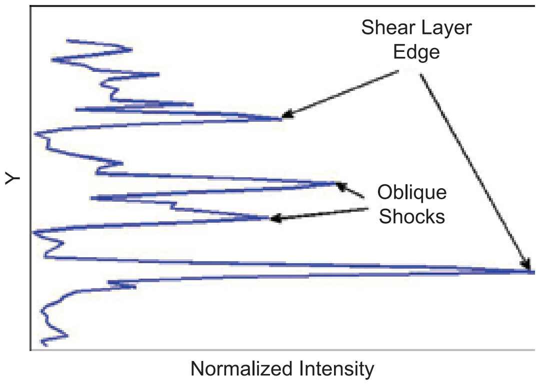

Figure 12: Intensity profile at 5 mm from the exit of the nozzle.

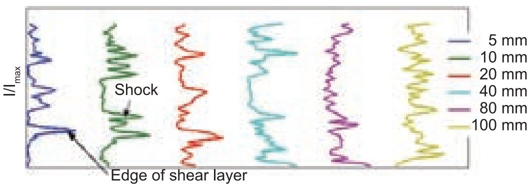

Figure 13: Progression of normalized intensity profiles for the edge enhanced schlieren image.

case. From Figure 13 also it can be seen that the non-mixed length is between 80 mm–100 mm. The unit of length in an image is pixel while the physical unit is in mm, this conversion can be carried out by finding the scale of the image using a reference length in the image which in this case is the duct height of 20 mm.

Discussion in this section has focused on the schlieren method of flow visualization, setting it up for the best images taken in time resolved manner with a high speed camera. The criterion for mixing is the increase in density of lines along the length of the ejector in an edge enhanced image. However, this method does not distinguish between the two flows at all, as the schlieren image is a density gradient image. The criterion is based on the presence of certain flow structures which are generally present in such flows. A clear evidence of mixing can be achieved by using a tracer and then looking at the spread of the tracer along the length of the ejector, which is done by seeding acetone vapors into the primary flow and then capturing the scattered light from a sheet of laser by condensed droplets of acetone, as described in the following.

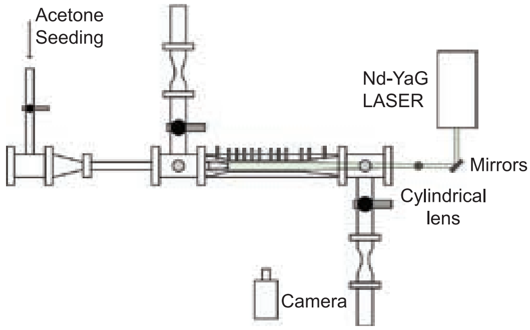

Figure 14: The optical arrangement for the laser scattering flow visualization technique.

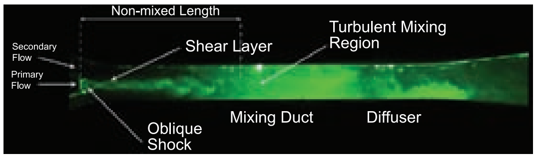

Figure 15: Instantaneous laser scattering image of the flow at a primary stagnation pressure P_{op} of 9.69 bar and entrainment ratio $\omega = 0.24$.

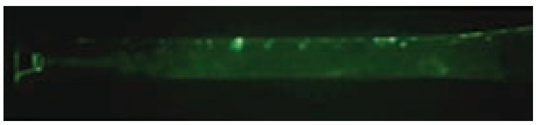

Figure 16: Instantaneous laser scattering image of the flow at a primary stagnation pressure P_{op} of 5.69 bar and entrainment ratio $\omega = 0.63$.

4 Flow Visualization Using Laser Scattering

In an ejector there are two flows present that undergo mixing; in a schlieren picture the overall density gradients are captured which can depict features like shocks, expansions, shear layers and turbulent zones, however, it does not distinguish one flow from the other. This demands that one flow be clearly marked from the other, which is done by seeding the primary flow with acetone vapors. A sheet of laser is passed into the ejector at midplane. When the primary flow expands in the supersonic nozzle, the resulting drop in pressure and temperature causes condensation of acetone into tiny droplets which scatter the intense plane of laser light into the transverse direction where it is captured by a camera. A Spectra Physics Quantaray Nd-YaG laser giving three wavelengths—1024 nm, 532 nm and 266 nm is used as the source of laser light. The 532 nm wavelenth is used with an energy of 180 mJ, having a pulse width of 7 ns and pulse rate of 10 Hz. The ejector setup has a glass window at the end flange. The laser beam of 10 mm diameter is first brought in line to the ejector flow direction by the use of suitable plane mirrors and is then rendered into a sheet using cylindrical lens. The sheet passes into the ejector flow passage through the glass window at the end flange of the ejector, along the flow direction at midplane. The scattering images are captured using the same Phantom camera. Acetone is seeded by bubbling nitrogen from a compressed gas cylinder through a reservoir that contains acetone liquid-vapor mixture, nitrogen carries vapors of acetone with it into the stagnation chamber of the primary flow. Similar to the schlieren technique the best configuration is arrived at by conducting series of experiments; good seeding was produced for nitrogen cylinder pressure of about 10 bar. Image of reasonable brightness could be obtained for laser powers greater than 180 mJ, hence it has been kept at the least. Only images fit for analysis are shown here since at non-optimal conditions the images were dark. The physics of condensation also plays a role in getting a good image. Figure 14 is a diagrammatic representation of the optical arrangement for the laser scattering.

Figure 15 is the instantaneous raw laser scattering image for the same conditions as the schlieren image with the primary flow seeded with acetone. Here the primary flow that has been seeded with acetone which condenses to droplets, gets emphasized, and as the droplets spread due to mixing, the intensity of scattered light spreads finally engulfing the whole height of the duct. In this image only the first shock in the primary flow is sharply visible where as the schlieren image shows a shock train of five shock cells.

Figure 16 is a laser scattering image at P_{op} = 5.69 bar and ω = 0.63, it is evident that the intensity of scattered light is less than the previous case. This is because the conditions across the nozzle i.e. stagnation pressure ratio, does not allow a full expansion, hence higher pressure and temperatures in the flow thus a reduction in condensation consequently a reduction in the density of droplets that scatter laser light. The fact that expansion is less can be observed in the schlieren image (Figure 17) where the primary jet is not as penetrative nor does it have as many shock cells as compared to the case with primary stagnation pressure at 9.69 bar.

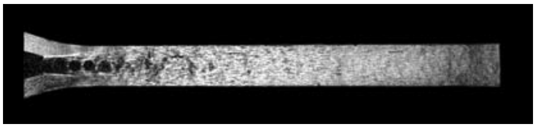

Figure 17: Instantaneous schlieren image of the flow at a primary stagnation pressure P_{op} of 5.69 bar and entrainment ratio $\omega = 0.63$.

Figure 18: The snapshot of the ejector at no flow condition.

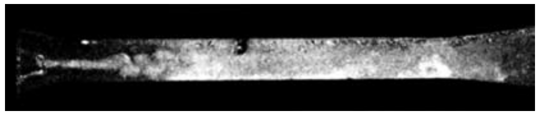

Figure 19: Figure 16 after background subtraction and contrast enhancement.

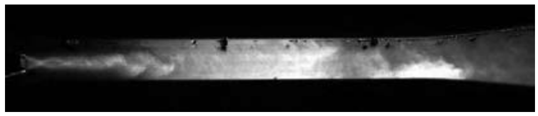

Figure 20: Figure 15 after background subtraction and contrast enhancement.

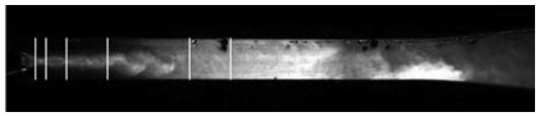

Figure 21: Superimposed image of lines along which intensity profiles are plotted in Figure 23.

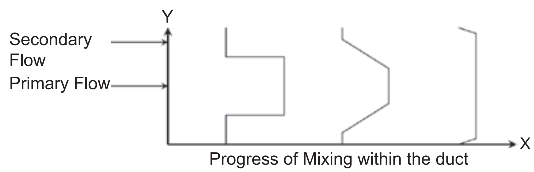

Figure 22: Schematic illustration of the progress of mixing within the duct.

Figure 23: Normalized intensity plots along the length of the ejector.

However, even in such a scenario with proper image processing it is possible to gather as much information as from the previous case.

4.1 *Image processing of laser scattering images*

Figure 18 is an image during the no flow condition of the ejector before the solenoid valve is opened. Notice that the image has a few background disturbance like the bright spots caused due to reflections from the top wall of the ejector. These are present even during flow with other minor background irregularities. These can be removed from the flow images by subtracting the no-flow image from the flow image so that only the effects caused because of the flow are highlighted, the quality is further enhanced by a contrast adjustment. The processing is carried out on the intensity images which are gray scale images devoid of color. The result of such an operation can be seen in the enhanced quality of Figure 16, an image with a low intensity and contrast to what can be seen in Figure 19. Figure 20 is the image of Figure 15 after undergoing the same procedure as above. These procedures only enhance the quality of the images and they depend on the quality of the captured image, hence though Figure 19 is a marked improvement over Figure 16, the original quality of Figure 15 being much crisper Figure 20 reflects the same. The point of interest in this study is the progress of mixing within the duct of ejector for which both images are equally suitable since both delineate the two flows.

Mixing in the duct proceeds from what is nearly a step, i.e. a distinct primary and secondary flow to a full or uniform profile as they approach a completely mixed scenario, the idealized version of which is shown in Figure 22.

The intensity profile variation along the length of the ejector on Figure 20 is evaluated by extracting the intensity data along vertical lines spanning the height of the ejector by using the MATLAB function improfile. Figure 23 shows the plot of normalized intensity with distance from the nozzle exit clearly following the trend shown in Figure 22.

Thus by scanning along the length of the ejector the location of non-mixed length can be found by identifying when the intensity profile changes from a peaky profile, as seen in the line 5 mm from the nozzle to a nearly uniform profile as in the line greater than 80 mm from the nozzle. This criterion is decided by ratio of mean of the profile to the peak of the profile; which is 1 for a uniform profile and minimum for a peaky profile. Based on this criterion the non-mixed length has been found to be 93 mm from the exit of the nozzle which if non-dimensionalized by the duct height comes out to be 4.65 L/D. Similar analyses are carried out on the schlieren image, but before taking the intensity profiles the image is rendered into an edge enhanced image by detecting the prominent edges using canny edge detection algorithm. Here, the larger number of edges are found in the mixing region while the non-mixed region has only a few edges corresponding to the shock and the shear layer, as shown in Figure 23. Estimation of the mixing length from the schlieren image comes out to be 99 mm which is 4.95 L/D.

4.2 *Experimental uncertainities*

There are various factors that affect the accuracy of these results primary among them is the discrete nature of the data being processed. The intensity profiles are available only upto the resolution of a pixel thus limited by the resolution of the camera and the optics. Good quality images are a function of flow itself and the dynamics of vapor condensation in such flows. Error is introduced when scaling the image from pixels to physical units since it depends on the exact acquisition of a reference length, which depends on placement of optics with respect to the experimental set up. The uncertainities associated with the discrete nature of the data and the canny algorithm amount to 5% while the scaling error gives a 3% uncertainity, combining the two, an overall 6% uncertainty in the results presented in this study. Within this experimental uncertainty the values of $L_{non-mixed}$ estimated from the laser scattering and schlieren are in good agreement.

5 Discussions and Conclusions

This article describes the application of two different techniques of flow visualization—schlieren and laser scattering to the experimental investigation of the mixing process within an ejector. The objective is to estimate the non-mixed length—length along the ejector for which the two flows are distinct using image processing of the images captured from the two complimentary techniques. The best optical arrangement giving clear sharp images of the flow are arrived at by doing a series of experiments. Instantaneous flow images at a primary stagnation pressure of 9.69 bar and 5.69 bar are shown with a qualitative description of the flow inferred from the images. Image processing tools of MATLAB are used to develop an in house code that is used to enhance the quality of images and extract the length of non mixed region from these images. In the case of schlieren technique, which produces an image proportional to density gradient, none of the two flows is marked and the non-mixed length is inferred from the development of flow structures i.e. density of lines caused due to turbulent mixing. Hence, the need to seed the primary flow with acetone thereby clearly marking it and estimating the mixing by the progress of spread of acetone particles from the primary flow. The length of non mixed region is established by locating the point where the intensity profile across the height of the mixing duct changes from a predominant peaky profile to a uniform profile. This estimation from the laser scattering images yields a 4.65 L/D for the case with stagnation pressure ratio of 9.69 bar and from the schlieren images of the same case it is 4.95 L/D. The fact that vapor condensation plays a crucial role in the efficacy of laser scattering images is brought by the comparison of the two cases. Given the sources of uncertainties due to optical arrangements, camera resolution and algorithm, the two methods are in good agreement. The analysis of the laser scattering images is restricted by the laser pulse rate of 10 Hz, which does not allow time-resolved study of the structures in the flow. However, having established that schlieren images give as much information about mixing as the laser scattering images, time resolved schlieren analysis can be used to determine their behavior. The ejector test rig facility has the flexibility for testing different geometries of ejectors and nozzles for mixing enhancement using the above developed technique.

Acknowledgements

The authors would like to thank M/s Tata Motors and DRDO New Delhi for financial support for the present study. The authors would also like to thank all the staff and students who helped during the course of the study.

Received 15 February 2013.

References

1. Anderson, J., *Modern Compressible Flow*, Mc-Graw Hill, 2004.
2. Chunnanond, K. and Aphornratana, S., "Ejectors: applications in refrigeration technology," *Renewable and Sustainable Energy Reviews*, Vol. 8, 2004, pp. 129–155.
3. Huang, B., Jiang, C., and Hu, F., "Ejector Performance Charateristics and Design Analysis of Jet Refrigeration System," *Journal of Fluids Engineering, Trans. ASME*, Vol. 107, July 1985, pp. 792–802.
4. Sun, D.-W. "Variable Geometry Ejectors and their Applications in Ejector Refrigerator Systems," *Energy*, Vol. 21, No. 10, 1996, pp. 919–929.

5. Ferrari, M.L., Bernardi, D. and Massardo, A.F. "Design and Testing of Ejectors for High Temperature Fuel Cell Hybrid Systems," *Journal of Fuel Cell Science and Technology, Trans. ASME*, Vol. 3, August 2006, pp. 284–291.
6. Alperin, M. and Wu, J.-J. "Thrust Augmenting Ejectors Part I," *AIAA Journal*, Vol. 21, No. 10, October 1983, pp. 1428–1436.
7. Alperin, M. and Wu, J.-J. "Thrust Augmenting Ejectors Part II," *AIAA Journal*, Vol. 21, No. 12, December 1983, pp. 1698–1706.
8. Francher, R.B., "Low-Area Ratio, Thrust-Augmenting Ejectors," *Journal of Aircraft*, Vol. 9, No. 3, March 1972, pp. 243–247.
9. Hickman, K.E., Gilbert, G.B. and Carey, J.H. *Analytical and Experimental Investigation of High Entrainment Ratio Jet Pumps*, NASA, 1970.
10. Annamalai, K., Satyanarayana, T.N.V., Sriramulu, V. and Bhaskaran, K.A. "Development of design methods for short cylindrical supersonic exhaust diffuser," *Experiments in Fluids*, Vol. 29, 2000, pp. 305–308.
11. Keenan, J., Neumann, E. and Lustwerk, F. "An Investigation of Ejector Design by Analysis and Experiment," *Journal of Applied Mechanics*, September 1950, pp. 299–309.
12. Fabri, J. and Paulon, J. *Theory and Experiment on Supersonic Air-to-Air Ejectors*, NACA, 1958.
13. Addy, A., Dutton, J. and Mikkelensen, C. *Supersonic Ejector-Diffuser Theory and Experiment*, University of Illinois Urbana, 1981.
14. He, S., Li, Y. and Wang, R. "Progress of mathematical modeling on ejectors," *Renewable and Sustainable Energy Reviews*, Vol. 13, No. 8, October 2008, pp. 1760–1780.
15. Huang, B., Chang, J. and Petrenko, V. "A 1-D Analysis of Ejector Performance," *International Journal of Refrigeration*, Vol. 22, 1999, pp. 354–364.
16. Rao, M.V.S. and Jagadeesh, G. "Vector evaluated particle swarm optimization (VEPSO) of supersonic ejector for hydrogen fuel cells," *Journal of Fuel Cell Science and Technology*, Vol. 7, No. 4, 2010, pp. 0410141–0410147.
17. Bartosiewicz, Y., Aidoun, Z., Desevaux, P. and Mercadier, Y. "Numerical and Experimental Investigations on Supersonic Ejectors," *International Journal of Heat and Fluid Flow*, Vol. 26, 2005, pp. 56–70.
18. Brown, G.L. and Roshko, A. "On density effects and large structure in turbulent mixing layers," *Journal of Fluid Mechanics*, Vol. 64, No. 4, 1974, pp. 775–816.
19. Papamoschou, D. and Roshko, A., "The Compressible Turbulent Shear Layer: an Experimental Study," *Journal of Fluid Mechanics*, Vol. 197, 1988, pp. 453–477.
20. Clemens, N.T. and Mungal, M.G., "Large-scale structure and entrainment in the supersonic mixing layer," *Journal Of Fluid Mechanics*, Vol. 284, 1995, pp. 177–216.
21. Dvorak, V. and Safarik, P. "Transonic instability in the Entrance Part of a Mixing Chamber of High-Speed Ejector," *Journal of Thermal Science*, Vol. 14, No. 3, 2005, pp. 260–271.
22. Ala Bouhanguel, P.D. and Gavignet, E. "Flow visualization in supersonic ejectors using laser tomography techniques," *International Journal of Refrigeration*, Vol. 34, 2011, pp. 1633–1640.
23. Desevaux, P., J.P.P. and Hostache, G. "An optical analysis of an induced flow ejector using light polarization properties," *Experiments in Fluids*, Vol. 16, 1994, pp. 165–170.
24. Merzkirch, W. *Flow Visualization*, Academic Press Inc., 1987.
25. Settles, G. *Schlieren and Shadowgraph Techniques*, Springer, 2001.
26. Gonzalez, R.C., Woods, R.E., and Eddins, S.L. *Digital Image Prossing using Matlab*, Gatesmark Publishing, 2009.
27. Kovesi, P.D. "MATLAB and Octave Functions for Computer Vision and Image Processing," Centre for Exploration Targeting, School of Earth and Environment, The University of Western Australia, 2000, Available from: <http://www.csse.uwa.edu.au/~pk/research/matlabfns/>.

M.V. Srisha Rao is currently a Ph.D. student in Department of Aerospace Engineering, Indian Institute of Science. He is currently working on the gas dynamics of internal compressible flows in a gaseous supersonic ejector. He has also been involved in studies on flow control in high speed flows, shock tube and shock tunnel investigations. His areas of interest include Fluid Mechanics, Gas Dynamics, Hypersonic Flow and Optical Diagnostics for Flow Measurement. He has over 10 articles including journal and conference proceedings. He has completed his ME from IISc, Bangalore.

G. Jagadeesh is a Professor in the Dept. of Aerospace Engineering, IISc—Bangalore. He is a fellow of Indian National Academy of Engineering and an Associate fellow of American Institute of Aeronautics and Astronautics. He is professionally associated with International Shock Wave Institute & Society for Shock Wave Research , India. He is Presently working on Hypersonic flow control using novel energy deposition methods; Supersonic mixing enhancement in ejectors; Shockwave propagation dynamics in complex fluids; New automated wave reactors for industrial and biomedical applications. His areas of interest include Experimental Hypersonics, Shock wave dynamics. He has published over 150 scientific papers in International journals and symposiums. He has completed his PhD from IISc Bangalore.